Wireless network capacity versus Ollivier-Ricci curvature under Heat Diffusion (HD) protocol.

Chi Wang, E. Jonckheere, and R. Banirazi

***Abstract*— Negative curvature in the relatively new Ollivier-Ricci sense of a wireless network graph is shown to be the culprit behind large queue occupancy, large routing energy, and restricted capacity region under any throughput optimal protocol. This is the wireless counterpart of the congestion phenomenon occurring in a Gromov negatively curved wired network under least cost path routing. Significantly different protocols call for significantly different curvature concepts to explain the "congestion" phenomenon. The rationale for the Ollivier-Ricci curvature is that it is defined in terms of a transportation cost—formalized under the Wasserstein distance—under a diffusion process. The Heat Diffusion protocol used in this paper is sensitive to the queue differential, so that interpreting packets as calories, it lends itself to a genuine heat diffusion, yet retaining the 3-stage process of weighting-scheduling-forwarding of Back-Pressure. The main result is that the transportation definition of the Ollivier-Ricci curvature allows for the direct connection—without resorting to the Laplacian operator of heat calculus—between curvature and queue occupancy, routing energy, and capacity region.**

I. Introduction

One of the great successes of the geometric approach to networks has been the explanation of the congestion phenomenon as resulting from least cost path routing on a Gromov hyperbolic graph [9]. Many of the classical graph generators, e.g., scale-free generator, representative of real networks have indeed been shown to have negative curvature properties [6]. It is a basic fact of differential geometry that on a negatively curved manifold the geodesics between uniformly distributed pairs of points have a tendency to pass through a "core" where the congestion is observed. Observe that we use a manifold argument to explain a graph phenomenon; this is an argument that has become popular over the past 10 years and justified by the common "coarse" geometric properties of Gromov negatively curved graphs and hyperbolic manifolds.

In wireless networks, the link interference adds extra difficulty relative to wireline networks. Under interference and link capacity constraints, the throughput optimality is crucially important in the context of limited wireless resources. Then the relevant protocol to address these issues is the Back-Pressure (BP) or a variation thereof. Different protocols call for different curvature concepts to explain the broader "congestion" concept of wireless networks: queue occupancy, the routing energy, or more generally the capacity region. The routing energy is the space-discrete version of the Dirichlet energy of heat diffusion on a manifold. By the Dirichlet principle, a protocol that minimizes routing energy would follow heat diffusion. In [1], we designed a protocol referred to as *Heat Diffusion (HD)*, which follows the heat diffusion process on a graph, yet keeping *weighting-scheduling-forwarding* structure of Back-Pressure.

The purpose of this paper is to identify the relevant graph topological features that are impacting queue occupancy, routing energy, and capacity region under heat diffusion. As argued in the following subsection, heat diffusion is regulated by the Ricci curvature or a coarse version thereof, the Ollivier-Ricci curvature. As main result, we show that the more negative the Ollivier-Ricci curvature, the higher the queue occupancy, the smaller capacity region.

A. Ollivier-Ricci curvature and heat diffusion

Given a heat equation solution $T(x,t)$ over a Riemannian manifold M endowed with a heat capacity measure dC, the heat measure $dQ = TdC$ is the solution of a continuity equation over the space $(\mathcal{P}_2(M), W_2)$ of probability measures defined over the Riemannian manifold M and endowed with the 2nd Wassertein metric W_2. In a bit the same way as sectional curvature regulates the divergence/convergence of the geodesics on the Riemannian manifold M, the (Ollivier-)Ricci curvature (coarsely) regulates the divergence/convergence of the heat diffusion paths in $(\mathcal{P}_2(M), W_2)$ (see [18]). For example, if P_t is the heat kernel over M and P_t^* the dual over $\mathcal{P}_2(M)$, we have $W_2\left(P_t^*Q_1, P_T^*Q_2\right) \leq e^{-Kt}W_2(Q_1,Q_2)$ where $0 \leq K \leq \mathrm{Ric}(M)$. It suffices to replace manifold by graph and think the probability measure defined on the vertices of a graph as the packet distribution to understand the role of the Ollivier-Ricci curvature.

Since the heat equation involves the Laplacian, one could think of establishing the curvature-diffusion connection via the Laplacian, as shown in Figure 1, and indeed Bauer [2] derived some bounds on the spectrum of the graph Laplacian in terms of the Ollivier-Ricci curvature. Another connection is the usual "second smallest eigenvalue" of the Laplacian related via Cheeger's theorem to the expansion coefficient. There is the folk statement that "high expansion coefficient" means negative curvature; however, this statement has recently been challenged by Ollivier [14] where in his Problem T, he proposes to find

> *"... a family of expanders (i.e., a family of graphs of bounded degree, spectral gap bounded away from* 0 *and diameter tending to* ∞*) with non-negative Ricci curvature."*

This work was supported by NSF grant NetSE 1017881.

Chi Wang, E. Jonckheere, and R. Banirazi are with the Department of Electrical Engineering, University of Southern California, Los Angeles, CA 90089 {wangchi, jonckhee, banirazi}@usc.edu

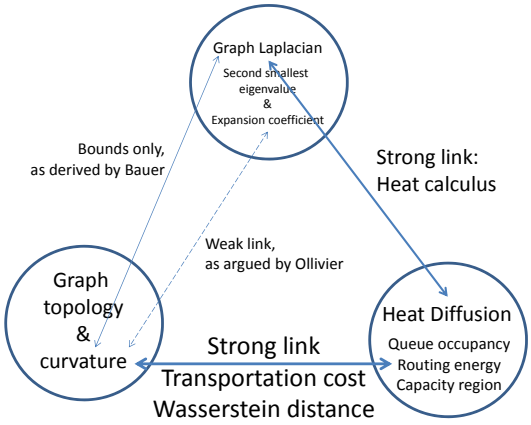

Fig. 1. Heat diffusion versus curvature versus graph Laplacian

In the same Figure 1, "Heat Diffusion" refers to a large body of mathematical work on how heat flows on a manifold (even a Finsler manifold) or a graph (even a directed graph) with its application to wireless networking inspired from heat diffusion. Naturally this leads to defining generalized Laplacian concepts, e.g., Laplacian on Finsler manifolds.

In the present paper, we develop the *direct* link between the performance of the Heat-Diffusion protocol and the curvature, as shown at the bottom of Figure 1. This connection is important because the Heat-Diffusion protocol is throughput optimal, so any relationship between Heat-Diffusion protocol and curvature means a connection between capacity region and curvature.

II. Wireless Network Thermodynamics

To formulate the Heat Diffusion (HD) policy, we associate with each d–packet flow a corresponding flow of heat on the network, for which node d is the only sink. In this analogy, the quantity of d-heat $Q_i^{(d)}$ at node i plays the role of the number of d–packets at the same node, where the d–temperature at node i is denoted by $T_i^{(d)}$.

The HD protocol works with the same algorithmic structure as ***Back-Pressure (BP)*** protocol, originally proposed by Tassiulas and Ephremides in 1992. There are two fundamental highlights in the way the BP is modified to become a genuine heat flow in the cast of HD [1].

- Contrary to BP, which transmits the maximum number of possible packets along each activated link, i.e., filling up the link capacity, HD limits the forwarding to be at most equal to one-half of the queue differential. This quality also has impact on the mitigation of queue oscillation and packet looping.
- The weighting w_{ij} of a link, which itself directly controls the scheduling, is taken quadratic rather than linear in the queue differential as practiced in BP. In view of this quality, the interference flow subject to the new protocol looks like, via the Dirichlet Principle, a suitably-weighted non-interference flow in the fluid limit, and hence a genuine heat flow. Thus the stability of the network can be analyzed using the ubiquitous heat calculus [12, Chap. 7], specialized to Finsler manifolds [5], from which it follows that hyperbolic networks are more difficult to stabilize. This is the natural follow up to the authors' long standing quest to understand the connection between congestion and curvature in *wired* networks [9]–[11], *wireless* networks [1], even quantum networks [7], [8].

A. Adiabatic link diffusion

Consider the nodes i and j as heat reservoirs with heat capacities C_i and C_j, resp., holding heat quantities $Q_i(n)$ and $Q_j(n)$, resp., at time slot n. The two reservoirs are connected by a conducting medium of infinitely large thermal conductivity and vanishingly small heat capacity, the latter to ensure that the heat exchange to uniformize the temperature is *adiabatic*. Then it is easy to calculate the number of calories transmitted from node i to node j as

$$f_{ij}^{\max}(n) = \max\left\{0,\ \left\lceil \frac{Q_i(n) - Q_j(n)}{2} \right\rceil \right\}, \qquad (1)$$

where $\lceil x \rceil$ returns the ceiling value of x. To make a protocol—in terms of packet rather than calorie flow—out of this basic heat transfer fact, $f_{ij}^{\max}(n)$ must be restricted to the ***link transmission rate*** $\mu_{ij}(n)$**.** Furthermore, the number of transmitted packets can be at most the number of packets that $Q_i(n)$ holds. Putting all of these together, the protocol can be devised as follows.

B. Thermodynamical Heat Diffusion (HD) protocol

At timeslot n, let $Q_i^{(d)}(n)$ denote the number of d-packets queued at the network layer of node i, and $f_{ij}^{(d)}(n)$ the *actual* number of d-packets transmitted via link ij, constrained by the link capacity $\mu_{ij}(n)$. HD is designed along the same 3-stage process as BP: *weighting-scheduling-forwarding.*

HD Weighting: At each timeslot n and for each link (i,j), the algorithm first finds the optimal d–packets to transmit as

$$Q_{ij}^{(d)}(n) = \max\left\{0,\ Q_i^{(d)}(n) - Q_j^{(d)}(n)\right\}, \qquad (2)$$
$$d_{ij}^*(n) = \arg\max_d Q_{ij}^{(d)}(n).$$

To attribute a weight to each link, the HD algorithm performs the following:

$$\widehat{f_{ij}}(n) = \min\left\{\left\lceil 1/2\ Q_{ij}^{(d^*)}(n)\right\rceil,\ Q_i^{(d^*)}(n),\ \mu_{ij}(n)\right\}, \qquad (3)$$

$$w_{ij}(n) = \left(\widehat{f_{ij}}(n)\right)\left(Q_{ij}^{(d^*)}(n)\right). \qquad (4)$$

Note that the left most term inside the braces of (3) is equivalent to (1) for d^*–packet. Observe that the weight (4) in HD is *quadratic* in queue differential. This contrasts with the BP policy, which relies on a *linear* weighting strategy.

HD Scheduling: After assigning the optimal weight (4) to each link, the scheduling matrix $\boldsymbol{S}(n)$ is chosen in a scheduling set $\boldsymbol{\mathcal{S}}$ by solving a centralized optimization problem as

$$\boldsymbol{S}(n) = \arg\max_{\boldsymbol{S}\in\boldsymbol{\mathcal{S}}} \sum\nolimits_{(i,j)\in\mathcal{E}} \boldsymbol{S}_{(i,j)} w_{ij}(n)\sigma_{ij}(n), \qquad (5)$$

where $\sigma_{ij} = 1/\rho_{ij}$ denotes the link profit factor. Note that while (5) is the same as that of BP, the solution to (5) is different due to the difference in the weighting process. *Particular BP-HD discrepancies are:*

1) Including ***link cost*** $\rho_{ij}(n) = 1/\sigma_{ij}(n)$ in (5), the HD algorithm gives priority to the links of lowest penalty, when possible to keep network stable.
2) Weighting based on the actual number of transmittable packets $\widehat{f_{ij}}(n)$ in (4), in lieu of $\mu_{ij}(n)$ in BP, attempts to optimize the routing performance in light and moderate traffic rates. As an example, consider two links a and b with differential queue backlogs of 1 and 3, and link transmission rates of 10 and 3, respectively. So the consequence of activating link a is transmission of 1 packet, versus 3 packets for link b. Observe that BP selects link a, while HD chooses link b.

HD Forwarding: Subsequent to the scheduling stage, each activated link transmits $\widehat{f_{ij}}\ (n)$ number of packets in accordance with (3). The rest of queues at node i are awaited for the next timeslots. Despite the BP policy that forwards the maximum possible number of d^*–packets across activated links, here packet forwarding is governed by diffusion mechanism, which also mitigates the *packet looping* behavior of BP. As an example, consider a network with only 2 packets at node i and no new arrivals. Let bidirectional link ij be of the highest transmission rate, and greater than 2, among all links connected to nodes i and j. BP loops these two packets between nodes i and j forever, while HD once transmits one of the packets to node j and then waits for new arrivals.

C. Stability and performance of HD protocol

The dynamics of the queue length process for d-packets at node i is described as

$$Q_i^{(d)}(n+1) = Q_i^{(d)}(n) - D_i^{(d)}(n) + E_i^{(d)}(n), \quad (6)$$

$$D_i^{(d)}(n) = \sum\nolimits_{b\in \mathrm{out}(i)} f_{ib}^{(d)}(n), \quad (7)$$

$$E_i^{(d)}(n) = A_i^{(d)}(n) + \sum\nolimits_{a\in \mathrm{in}(i)} f_{ai}^{(d)}(n), \quad (8)$$

where $D_i^{(d)}(n)$ and $E_i^{(d)}(n)$ represent the total number of d-packets departed from and arrived at node i, respectively, in the timeslot n, and $\mathrm{out}(i)$ and $\mathrm{in}(i)$ denote the sets of outgoing and incoming neighbors of node i, respectively.

Definition 1 (Network Stability): A queue $Q_i^{(d)}(n)$ is stable, if $\limsup_{n\to\infty} \mathbb{E}\{Q_i^{(d)}(n)\} < \infty$. A network is stable if all its queues are stable.

Definition 2 (Capacity Region): Given a routing policy, its *stability region* is the set of all traffic rate matrices that can be stabilized by it. Network *capacity region* $\mathbf{\Lambda}$ is the union of the stability regions achieved by all possible routing policies, including those of perfect precognition about random events.

Definition 3 (Throughput-Optimal Policy): A routing policy is throughput-maximal, if it stabilizes all *admissible* traffic rate matrices $\boldsymbol{\lambda} \in \mathbf{\Lambda}$.

Proposition 1 (Throughput-Optimal Policy): Consider a routing network with N wireless nodes. The HD routing algorithm stabilizes the network for any traffic rate matrix $\boldsymbol{\lambda}$ strictly interior to the network capacity region $\mathbf{\Lambda}$.

Proof: For simplicity, we consider only one destination node in the network. We further assume $\rho_{ij} = 1$ for all links. Consider a Lyapunov energy function $V(n) = 1/2\sum_i Q_i(n)^2$ and define Lyapunov drift $\Delta V(n) = V(n+1) - V(n)$. Some mathematical manipulation yields

$$\Delta V = \sum\nolimits_i \Big[\frac{1}{2}(E_i^2 + D_i^2) + Q_i(E_i - D_i) - E_i D_i\Big].$$

From (7) and (8) we obtain

$$\Delta V \le BN + \sum\nolimits_i Q_i A_i - \sum\nolimits_i Q_i \sum\nolimits_{a,b}(f_{ib} - f_{ai}), \quad (9)$$

$$B = \frac{1}{2N}\sum\nolimits_i \Big[(A_i^{\max} + \sum\nolimits_a \mu_{ai}^{\max})^2 + (\sum\nolimits_b \mu_{ib}^{\max})^2\Big],$$

where constant $\mu_{ij}^{\max}$ stands for a deterministic upper bound on $\mu_{ij}(n)$. Since $\boldsymbol{\lambda}$ is assumed strictly interior to the capacity region $\mathbf{\Lambda}$, there exists a vector $\boldsymbol{\epsilon}$ with positive entries such that $\boldsymbol{\lambda} + \boldsymbol{\epsilon} \subseteq \mathbf{\Lambda}$. Therefore, there exists a randomized routing policy which stabilizes $\boldsymbol{\lambda}$ based only on the current topology state and so independent of the queue occupancies. Also for any stabilizable traffic rate, there exists a hyper-flow in long-term average such that

$$\mathbb{E}\Big\{\sum\nolimits_{a,b}(f'_{ib} - f'_{ai})\Big\} = \lambda_i + \epsilon_i \quad (10)$$

for some f'_{ib} and f'_{ai}. It is proven that the HD policy minimizes the Lyapunov drift (9) compared to any other policy including BP. Also observe that

$$\sum\nolimits_i Q_i \sum\nolimits_{a,b}(f_{ib} - f_{ai}) = \sum\nolimits_{(i,j)} f_{ij}(Q_i - Q_j).$$

Considering these two facts, taking conditional expectation with respect to $\boldsymbol{Q}(n)$ from (9), and using (10) yield

$$\mathbb{E}\left\{\Delta V |\, \boldsymbol{Q}\right\} \le BN - \sum\nolimits_i Q_i \epsilon_i.$$

Defining $\|\boldsymbol{Q}\| = \sum_i Q_i$ and $\delta = \min_i(\epsilon_i)$ gives

$$\mathbb{E}\left\{\Delta V |\, \boldsymbol{Q}\right\} \le BN - \delta\|\boldsymbol{Q}\|. \quad (11)$$

Hence, for $\|\boldsymbol{Q}\| > BN/\delta$, we get $\mathbb{E}\{\Delta V |\, \boldsymbol{Q}\} < 0$, and thus the queuing system is stable. ∎

Now assume that time is continuous and the evolution of each queue is governed by the following differential equation:

$$\dot{\widetilde{Q}}_i^{(d)} = -\sum\nolimits_{b\in \mathrm{out}(i)} \widetilde{f}_{ib}^{(d)} + \sum\nolimits_{a\in \mathrm{in}(i)} \widetilde{f}_{ai}^{(d)} + \lambda_i^{(d)}, \quad (12)$$

for all $i, d = 1, \ldots, N$, where dot on the top denotes the continuous-time derivative. The HD algorithm assigns link rates at every instant of time as described. Then, the following asymptotic stability result holds.

Proposition 2 (Time Average Convergence): The states of the continuous-time system (12) asymptotically converges to the states of a traditional heat diffusion on a directed graph with edge weights of $\sigma_{ij} = 1/\overline{\rho_{ij}}$, where $\overline{\rho_{ij}}$ denote the long-term averages of ρ_{ij}.

Proof: We give a sketch of the proof only for one destination node with $\rho_{ij} = 1$. We indicate variables in the traditional heat diffusion system with superscript $*$. Consider

a node energy function as $V(i) = 1/2(\widetilde{Q}_i - \widetilde{Q}_i^*)^2$. Taking derivative, and substituting from (12) yield

$$\dot{V}(i) = \lambda_i(\widetilde{Q}_i - \widetilde{Q}_i^*) - \widetilde{Q}_i \sum\nolimits_b \widetilde{f}_{ib} + \widetilde{Q}_i^* \sum\nolimits_b \widetilde{f}_{ib} + \widetilde{Q}_i \sum\nolimits_a \widetilde{f}_{ai} - \widetilde{Q}_i^* \sum\nolimits_a \widetilde{f}_{ai}.$$

Since λ_i is considered as the same input to both routing network and traditional heat graph,

$$\lambda_i = \sum\nolimits_b \sigma_{ib}\widetilde{Q}_{ib}^* - \sum\nolimits_a \sigma_{ai}\widetilde{Q}_{ai}^*,$$

where $\widetilde{Q}_{ij}^* = \max\left\{0,\ \widetilde{Q}_i^* - \widetilde{Q}_j^*\right\}$. Using these equations in $\dot{V}(i)$ and summing up over all nodes,

$$\begin{aligned}\dot{V} &= \sum\nolimits_{(i,j)} \Big[\widetilde{f}_{ij}(\widetilde{Q}_i^* - \widetilde{Q}_j^*) - \widetilde{f}_{ij}(\widetilde{Q}_i - \widetilde{Q}_j) \\ &\qquad + \sigma_{ij}\widetilde{Q}_{ij}^*(\widetilde{Q}_i - \widetilde{Q}_j) - \sigma_{ij}\widetilde{Q}_{ij}^*(\widetilde{Q}_i^* - \widetilde{Q}_j^*)\Big] \\ &= \sum\nolimits_{(i,j)} (\sigma_{ij}\widetilde{Q}_{ij}^* - \widetilde{f}_{ij}) \underbrace{\left((\widetilde{U}_i - \widetilde{U}_i^*) - (\widetilde{U}_j - \widetilde{U}_j^*)\right)}_{M}.\end{aligned}$$

Manipulating (2)–(5), one can see that if $M > 0$, then $\widetilde{f}_{ij} > \sigma_{ij}\widetilde{Q}_{ij}^*$ and so $\dot{V} < 0$. Also if $M < 0$, it can be shown that necessarily $\widetilde{f}_{ij} < \sigma_{ij}\widetilde{U}_{ij}^*$ and so $\dot{V} < 0$. These imply that $\lim_{t\to\infty} V \to 0$, and equivalently $\lim_{t\to\infty} \widetilde{Q}_i \to \widetilde{Q}_i^*$, which concludes the proof. ∎

III. Ollivier-Ricci curvature

In the wake of the newly formulated concept of *Ollivier-Ricci curvature [2], [13]*, heat calculus was redirected towards the connection between the heat kernel (related to graph Laplacian) and the new curvature concept (see, e.g., [4] and the work of Gregoryan) . However, here, our interest in the Ollivier-Ricci curvature rather stems from it very definition in terms of a "transportation cost," which can be linked to queue occupancy, routing cost, even time to reach steady-state.

Consider a weighted graph $((\mathcal{V}, \mathcal{E}), \rho)$. On this graph, for each vertex i, we define a probability measure m_i on $\mathcal{N}(i)$ as follows:

$$\begin{aligned} m_i(j) &= \frac{\rho_{ij}}{\sum_{j\in\mathcal{N}(i)} \rho_{ij}}, \quad \text{if } ij \in \mathcal{E} \\ &= 0, \quad \text{otherwise.}\end{aligned}$$

In full agreement with the recent work on network traffic versus graph curvature [9], [11], the Ollivier-Ricci curvature is defined in terms of the transport properties of the graph:

Definition 4: The Ollivier-Ricci curvature of the graph $((\mathcal{V}, \mathcal{E}), \rho)$ endowed with the set of probability measures $\{m_i : i \in \mathcal{V}\}$ is defined, along the path $[i, j]$, as

$$\kappa([i,j]) = 1 - \frac{W_1(m_i, m_j)}{d(i,j)}, \tag{13}$$

where $W_1(m_i, m_j)$ is the first Wasserstein distance between the probability measures m_i and m_j defined on $\mathcal{N}(i)$ and $\mathcal{N}(j)$, resp.,

$$W_1(m_i, m_j) = \inf_{\xi^{ij}} \sum_{k,\ell\in\mathcal{N}(i)\times\mathcal{N}(j)} d(k,\ell)\xi^{ij}(k,\ell),$$

where the infimum is extended over all "coupling" measures ξ^{ij} defined on $\mathcal{N}(i) \times \mathcal{N}(j)$ and projecting on the first (second) factor as m_i (m_j), that is,

$$\sum_{\ell\in\mathcal{N}(j)} \xi^{ij}(k,\ell) = m_i(k), \quad \left(\sum_{k\in\mathcal{N}(i)} \xi^{ij}(k,\ell) = m_j(\ell)\right)$$

and $d(i, j)$ is the usual metric emanating from the edge weight ρ.

More intuitively, $\xi^{ij}(k, l)$ is called *transference plan.* It tells us how much of the mass of $k \in \mathcal{N}(i)$ is transferred to $l \in \mathcal{N}(j)$, but it does not tell us about the actual path that the mass has to follow. Ollivier [13] showed that (13) ties up with the usual Ricci curvature on manifolds and δ-hyperbolic spaces.

The first Wasserstein distance is one class of shortest transportation distance between two probability distributions. For details of this concept, see [16], [17]. Note that we can define the p-Wasserstein metric

$$(W_p(m_i, m_j))^p = \inf_{\xi^{ij}} \sum_{k,\ell\in\mathcal{N}(i)\times\mathcal{N}(j)} (d(k,\ell))^p \xi^{ij}(k,\ell).$$

From here on, we shall restrict the definition to edges instead of paths. The specialization of (13) to edges is trivial and left to the reader. The first result of the edge-specialized concept is that W_1 satisfies the triangle inequality,

$$W_1(ij) + W_1(jk) \geq W_1([i,k]).$$

It follows that, if we take $\rho_{ij} = 1$,

$$\frac{1}{2}\left(\kappa(ij) + \kappa(jk)\right) \leq \kappa([i,k]).$$

Therefore, it is enough to evaluate the curvature between two neighboring points [13, Proposition 19] to derive lower bounds on the Ollivier-Ricci curvature.

Bauer [2] developed a general sharp inequality for undirected, weighted, connected, finite (multi)graph of N vertices $\mathcal{G} = (\mathcal{V}, \mathcal{E})$ as follows:

$$\begin{aligned}\kappa(ij) \geq & \\ &-\left(1 - \frac{\rho_{ij}}{d_x} - \frac{\rho_{ij}}{d_j} - \sum_{i_1, i_1\sim i, i_1\sim j} \frac{\rho_{i_1 i}}{d_i} \vee \frac{\rho_{i_1 j}}{d_i}\right)_+ \\ &-\left(1 - \frac{\rho_{ij}}{d_x} - \frac{\rho_{ij}}{d_j} - \sum_{i_1, i_1\sim i, i_1\sim j} \frac{\rho_{i_1 i}}{d_i} \wedge \frac{\rho_{i_1 j}}{d_i}\right)_+ \\ &+ \sum_{i_1, i_1\sim i, i_1\sim j} \frac{\rho_{i_1 i}}{d_i} \wedge \frac{\rho_{i_1 j}}{d_i} + \frac{\rho_{ii}}{d_i} + \frac{\rho_{jj}}{d_i}. \end{aligned} \tag{14}$$

In the above, $a_+ = \max(a,\ 0)$; $a \bigwedge b = \min(a,\ b)$; $a \bigvee b = \max(a, b)$; $d_i = \sum_{j\sim i} \rho_{ij}$, ρ_{ii} is the weight of self-loops; $j \sim i$ denotes the existence of an edge between j and i.

The connection between the Ollivier-Ricci curvature and the graph Laplacian is developed in [2] and not reproduced here.

IV. Ollivier-Ricci Curvature of Standard Graph Generators versus Network Stability: single class network and curvature lower bound

The HD protocol simulation is setup as follows:

- **Graphs used**. A total of 9 different graphs of the same order ($|V| = 50$) are used to relate the Ollivier-Ricci curvature and the performance of the HD protocol that runs on the graphs. Those graphs are
  - a complete graph,
  - three scale-free random graphs with different growth parameter,
  - three Erdös-Rényi random graphs with different attachment probabilities, generated by MIT Matlab Network Analysis toolbox [3],
  - two small-world random graphs generated by Watts-Strogatz model (k-nearest neighbors connection with $k = 3, 4$, respectively, rewiring probability is 0.2).
- **Link capacity**. For the queue occupancy and the routing energy, the link capacity is set to infinity. For the capacity region in the next section, the link capacity is set to 1500 packets for every link.
- **Packet arrival rate.** Except for the simulation related to the capacity region, in order to avoid random effects and to single out the specific impact of the network topology, the packet arrival rate is set to 1 Packet per Timeslot (PpT) from every node to one single sink (single-class) or to every other node (multi-class).
- **Scheduling.** It is known that for K-hop interference model for $K > 1$, the maximum weighted matching problem is NP-hard. For $K = 1$, however, the problem is polynomial-time solvable. One algorithm one would mention is Edmonds' blossom algorithm. The weighting in our simulation is provided by the quadratic weight (4) along edges. The maximum weighted matching algorithm at each timeslot is used to solve (5).
- **Position of the sink.** In single-class HD protocol, the position of the sink is chosen at random. However, different positions of the sink should result in different simulation results. Therefore, in the next section, an unbiased model using *multi-class* HD protocol is used to rule out the effect brought by the position of the sink.
- **Outline of simulation**. Essentially, we link congestion to curvature. The congestion of the network is reflected in two measurements:
  - the average queue occupancy over all nodes, $\frac{1}{|V|}\sum_{i\in V} Q_i(n)$;
  - the average routing energy over all links, $\frac{1}{|E|}\sum_{i,j\in E}\frac{1}{2}(Q_i(n) - Q_j(n))^2$.

  Curvature is measured in two different ways:
  - as the average of the lower bound on the Ollivier-Ricci curvature over all edges;
  - as the exact Ollivier-Ricci curvature averaged over all edges (next section).

  Two different setups are considered on all nine different graph models:

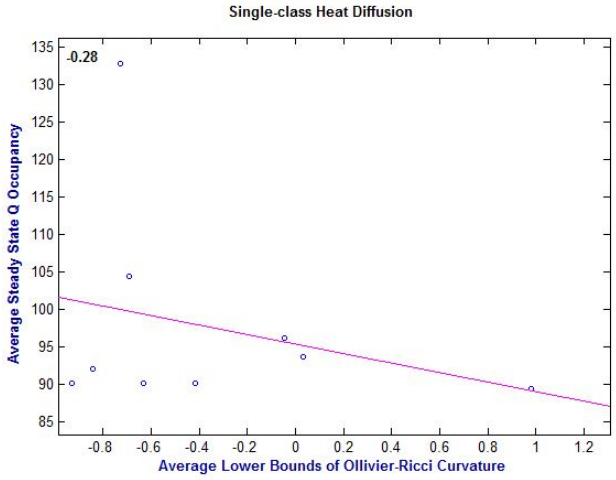

Fig. 2. Single class: queue occupancy averaged over all nodes in steady state versus lower bounds of Ollivier-Ricci curvature averaged over all links in each of the 9 graphs. (The red line is the least square error linear interpolation of the queue occupancy versus the curvature.)

  - the single-class (5,000 timeslots in total are run);
  - the multi-class (20,000 timeslots in total are run in the next section). The multi-class has been proved to be the superposition of single-class heat diffusions in steady-state.

We use MATLAB R2012a to perform all the simulations. Scheduling is based on the Blossom Algorithm; weighting and forwarding are both based on the HD protocol. The heat capacity is set as $C_i(n) = 1,\ \forall i, \forall n$. At timeslot 0, the heat quantity is set to 0 for every node.

A. Queue occupancy versus Ollivier-Ricci curvature

The Ollivier-Ricci curvature estimate used in the simulations is the lower bound (14) on the curvature averaged over all edges. The steady-state queue occupancy of the network increases as Ollivier-Ricci curvature of the graph decreases as shown in Figure 2, although not monotonically, yet the slope of the interpolation line is -0.28.

B. Average routing energy versus Ollivier-Ricci curvature

The routing energy on the edge ij is defined as $E_K(ij) = \frac{1}{2}(Q_i(n) - Q_j(n))^2$ for n in steady-state regime. If the routing energy is averaged over all edges, $E_K = \frac{1}{|E|}\sum_{i,j\in E}\frac{1}{2}(Q_i(n) - Q_j(n))^2$, we have a global metric, which should be related to the Ollivier-Ricci curvature of the graph, as Figure 3 indeed shows. The routing energy increases with decreasing curvature with a slope of -0.23, as expected.

Although the Ollivier-Ricci curvature and the network congestion are not monotonically related, they still show a correlation. The reason of the low correlation value mainly comes from two sources. The first is that the result of single-class heat diffusion depends on the position of the sink, which is chosen at random in the simulation. The second is that the lower bound on Ollivier-Ricci curvature is still an

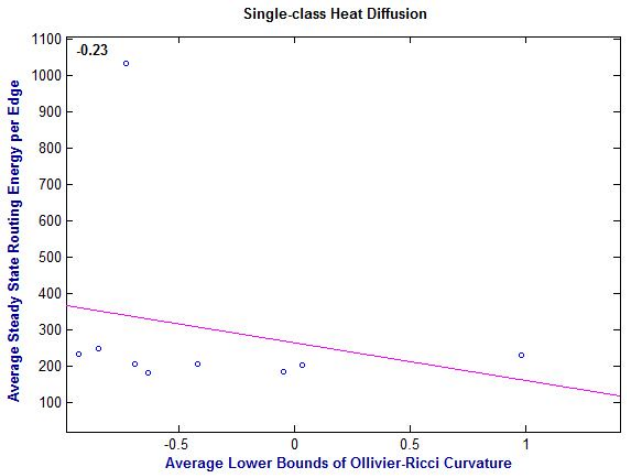

Fig. 3. Single class: average routing energy in steady state versus lower bounds of Ollivier-Ricci curvature averaged over all links.

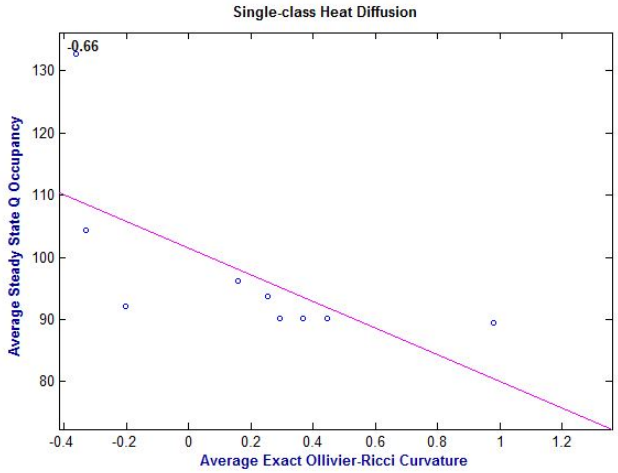

Fig. 4. Single-class: average queue occupancy in steady-state versus exact Ollivier-Ricci curvature averaged over all links.

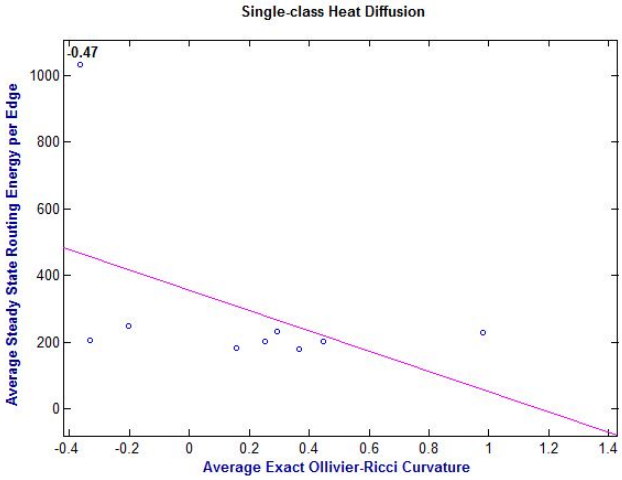

Fig. 5. Single-class: average routing energy in steady-state versus exact Ollivier-Ricci curvature averaged over all links.

estimate. (This situation will be rectified in the next section by computing the *exact* Ollivier-Ricci curvature.)

V. Ollivier Ricci Curvature of Standard Graph Generators versus Network Stability: single & multiple class network and exact curvature

The results based on the lower bound can be inaccurate in some cases. For example, for a Euclidean square lattice, for two neighboring nodes that are not on the boundary of the graph, the lower bound calculated by Bauer's equation is -1. However, the actual accurate value of the transportation distance is 1, which results in vanishing Ollivier-Ricci curvature. Thus, the actual congestion should reflect the vanishing of the curvature.

Based on the above concern, we need to calculate the *exact* Ollivier-Ricci curvature instead of a lower bound to further develop the congestion versus curvature relationship. One way to do the calculation is the utilization of the Earth Mover's Distance (EMD). EMD is a measure of the distance between two probability distributions, usually used in image processing [15]. It is based on the precise minimal cost to transform one distribution into the other. For accurate simulations, this minimal cost should be calculated by linear programming [2] as follows:

In the set-up of the original Monge-Kantorovich problem, let S denote the vector of supply and S_i denote the amount of supply at location i. Let D denote the vector of demand and D_j denotes the amount of demand at location j. We also have a cost matrix $\mathbf{C}$, where C_{ij} is the transportation cost of moving a unit mass from supply location i to demand location j. Let $x(i,j)$ denotes the amount of mass transported from i to j. In linear programming, we are minimizing the total cost

$$\text{Optimal Cost} = \min_{x(i,j)\geq 0} \sum_i \sum_j x\,(i,j)\,C(i,j),$$

subject to the constraints

$$\sum_j x\,(i,j)\,C(i,j) \leq S(i), \quad \sum_i x\,(i,j)\,C(i,j) \leq D(j).$$

Linear programming allows the extension of this computation method for symmetric directed graphs to general directed graphs.

A. Congestion of HD protocol versus exact Ollivier-Ricci curvature with improvements

Based on the same simulation setup as in the previous section, we now relate the congestion of single-class HD protocol with the *exact* Ollivier-Ricci curvature.

From the results (Figures 4-5), we see that the correlation between exact Ollivier-Ricci curvature and congestion is significantly improved compared with the correlation between lower bound of Ollivier-Ricci curvature and congestion. This can be further improved by going to multi-class HD protocol (Figures 6-7). The simulation setup is basically the same.

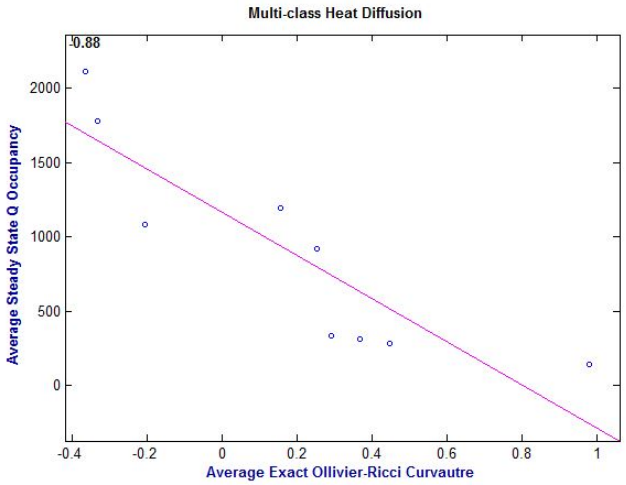

Fig. 6. Multi-class: average queue occupancy in steady-state versus exact Ollivier-Ricci curvature averaged over all links.

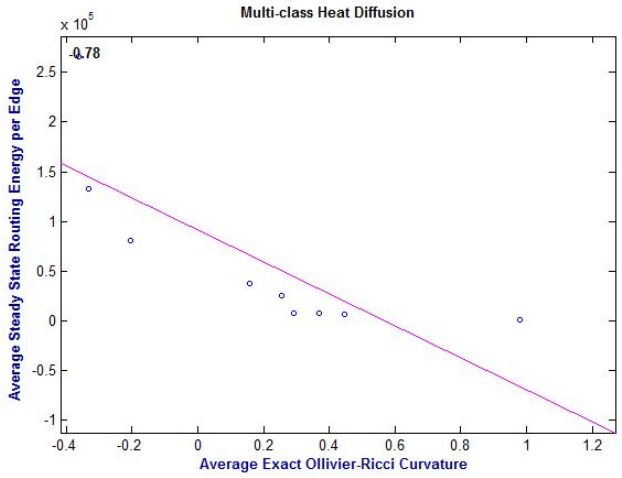

Fig. 7. Multi-class: average routing energy in steady-state versus exact Ollivier-Ricci curvature averaged over all links.

The only difference is that for each timeslot, every node is sending 1 packet to every other node instead of only 1 specific sink.

B. Network capacity region versus Ollivier-Ricci curvature

In this simulation, every graph is subject to different arrival rates. Previously, all nodes had an arrival rate of 1 PpT (packet per timeslot). Here, in this simulation, the arrival rate is uniformly increased to 2 PpT, 3 PpT, 5 PpT and 10 PpT. The change of arrival rate is applied to every node. The link capacity is uniformly set to 1500 packet for every link. In order to compare the capacity regions under different arrival rates with different Ollivier-Ricci curvature, Figure 8 shows the initial curve of timeslot versus average queue occupancy. In Figure 8, the link capacity is still infinity and arrival rate is still 1 PpT.

From Figure 8, we can see that for graphs with different curvatures, it takes longer time for the networks with more

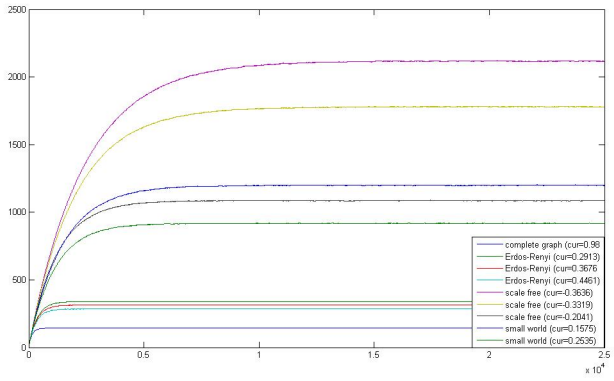

Fig. 8. Evolution of average queue occupancy with time under uniform arrival rate.

negative curvature to converge to steady-state. Also, the steady-state queue occupancy is higher in networks with more negative curvature, as also shown in Figure 6. However, no matter how long it takes to converge, they still converge within a finite amount of timeslots because the link capacity is infinity. This is not the case for the ones with finite link capacity.

Figure 9 show the performance with 1500 link capacity under different arrival rates of 2 PpT, 3PpT, 5PpT, and 10 PpT respectively.

We can make several observations from the Figure 9.

1) As the arrival rate goes higher, the graph with more negative curvature tends to lose convergence more rapidly than those with more positive curvature.

2) Under specific arrival rate, if the graph with more positive curvature cannot converge to steady state, then graphs with curvature less than that graph would not converge either. This demonstrates, although not a proof, that as the curvature of a graph is decreasing, the capacity region is also becoming smaller.

3) No matter what the arrival rate is, the time needed to reach steady-state and the steady-state average queue occupancy follow the same pattern as before, that is, they increase with decreasing curvature.

4) For any particular graph, if the arrival rate is increased, so will the time needed to reach steady-state.

Careful inspection of the various graphs being generated shows that the number of edges increases with the curvature, and trivially the capacity region increases. Simulations at constant number of edges still show that the capacity region increases with the curvature. However, the important feature is that the number of edges is only one of the factors contributing to the curvature; among other factors, one will mention the combinatorics of the edges and the link cost factors ρ_{ij}.

VI. Conclusion: Towards Ollivier-Ricci Curvature Control

In case the Ollivier-Ricci curvature is too negative for acceptable queue occupancy, one could think of chang-

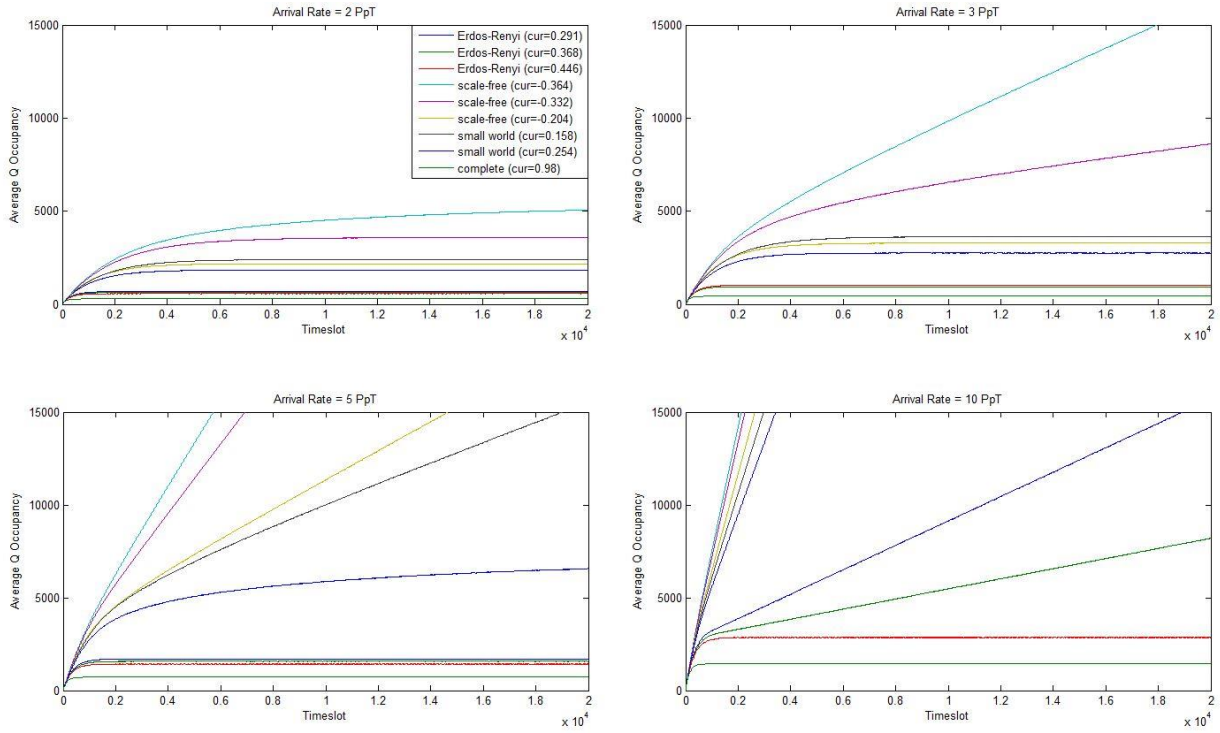

Fig. 9. Evolution of average queue occupancy with time under different arrival rates

ing the wireless parameters—within the constraints on the resources—in such a way as to increase the curvature, hence removing some of the overloaded queues and/or improving the capacity region. Such an approach has been very successful in wired networks, where the link weights are adjusted by the so-called Ricci flow to make the network of maximum curvature, under a given network combinatorics [10], [11]. Translated into wireless networking, this would mean changing the link cost factors ρ_{ij}, subject to the constrained resources, so as the maximize κ. However, in wireless networking, another variable to be manipulated is the combinatorics of the wireless channels. While this optimization is considerably more complicated than the wireline one, it is more flexible than the wireline one and hence would allow more curvature control authority. This is left for further research.

REFERENCES

[1] R. Banirazi, E. Jonckheere, and B. Krishnamachari. Heat diffusion algorithm for resource allocation and routing in multihop wireless networks. In *Globecom*, pages 5915–5920, Anaheim, Calfifornia, USA, December 3-7 2012. Session WN16: Routing and Multicasting.

[2] F. Bauer, J. Jost, and S. Liu. Olivier-Ricci curvature and the spectrum of the normalized graph Laplace operator. arXiv:1105.3803v1[math.CO] 19 May 2011, 2011.

[3] G. Bounova and O. L. de Weck. Overview of metrics and their correlation patterns for multiple-metric topology analysis on heterogeneous graph ensembles. *Phys. Rev. E*, 85:016117, 2012.

[4] J. Cheeger, M. Gromov, and M. Taylor. Finite propagation speed, kernel estimates for functions of the Laplace operator, and the geometry of complete riemannian manifolds. *J. Differential geometry*, 17:15–53, 1992.

[5] Shin ichi Ohta and Karl-Theodor Sturm. Heat flow on finsler manifolds. arXiv:0808.1166v4 [math.AP] 26 Sept 2012, 2012.

[6] E. Jonckheere, F. Ariaei, and P. Lohsoonthorn. Scaled Gromov four-point condition for network graph curvature computation. *Internet Mathematics*, 7(3):137–177, August 2011. DOI: 10.1080/15427951.2011.601233.

[7] E. Jonckheere, F. C. Langbein, and S. G. Schirmer. Curvature of quantum rings. In *Proceedings of the 5th International Symposium on Communications, Control and Signal Processing (ISCCSP 2012)*, Rome, Italy, May 2-4 2012.

[8] E. Jonckheere, S. Schirmer, and F. Langbein. Geometry and curvature of spin networks. In *IEEE Multi-Conference on Systems and Control*, pages 786–791, Denver, CO, September 2011. available at arXiv:1102.3208v1 [quant-ph].

[9] Edmond Jonckheere, Mingji Lou, Francis Bonahon, and Yuliy Baryshnikov. Euclidean versus hyperbolic congestion in idealized versus experimental networks. *Internet Mathematics*, 7(1):1–27, March 2011.

[10] M. Lou. *Traffic pattern analysis in negatively curved networks*. PhD thesis, University of Southern California, Los Angeles, CA, May 2008. Available at http://eudoxus.usc.edu/IW/Mingji-PhD-Thesis.pdf.

[11] M. Lou, E. Jonckheere, Y. Baryshnikov, F. Bonahon, and B. Krishnamachari. Load balancing by network curvature control. *International Journal of Computers, Communications and Control (IJCCC)*, 6(1):134–149, March 2011. ISSN 1841-9836.

[12] Richard Melrose. *The Atiyah-Patodi-Singer Index Theorem*, volume 4 of *Research Notes in Mathematics*. AK Pieters, Welesley, MA, 1993.

[13] Y. Ollivier. Ricci curvature on Markov chains on metric spaces. arXiv:0701886v4 [math.PR] 30 Jul 2007, 2007.

[14] Y. Ollivier. Discrete Ricci curvature: open problems. available at http://www.yann-ollivier.org/rech/publs/, May 2008.

[15] Y. Rubner, C. Tomasi, and L. Guibas. The earth movers distance as a metric for image retrieval. *International Journal of Computer Vision*, 40(2):00–121, 2000.

[16] C. Villani. *Topics in optimal transportation*, volume 58 of *Graduate Studies in Mathematics*. Providence, RI, 2003.

[17] C. Villani. *Optimal transport, Old and new*, volume 338 of *Grundlehren der Mathematischen Wissenschaften*. Springer-Verlag, Berlin, 2009.

[18] Max-K. von Renesse and Karl-Theodor Sturm. Transport inequalities, gradient estimates, entropy and ricci curvature. *Communications on Pure and Applied Mathematics*, 58(7):923–940, 2005.